

Interrelationships between regional blood flow, blood volume, and ventilation in supine humans

L. H. BRUDIN, C. G. RHODES, S. O. VALIND, T. JONES, AND J. M. B. HUGHES
Medical Research Centre Cyclotron Unit and Department of Medicine, Royal Postgraduate Medical School,
Hammersmith Hospital, London W12 0HS, United Kingdom

Brudin, L. H., C. G. Rhodes, S. O. Valind, T. Jones, and J. M. B. Hughes. Interrelationships between regional blood flow, blood volume, and ventilation in supine humans. *J. Appl. Physiol.* 76(3): 1205–1210, 1994. — Positron emission tomography was used to measure alveolar gas volume, pulmonary blood volume (V_B), regional alveolar ventilation (\dot{V}_A), and the regional ventilation-to-perfusion ratio (\dot{V}_A/\dot{Q}) in a transaxial slice at midheart level in eight supine subjects and one prone normal subject during quiet breathing. These relationships allow regional blood flow (\dot{Q}) to be calculated as $\dot{V}_A/(\dot{V}_A/\dot{Q})$. No significant differences between right and left lung were found. Within the volume studied, which excluded the peripheral 2 cm of the lung, there was an exponential increase in \dot{Q} by 11%/cm from 1.2 ml·min⁻¹·cm⁻³ in the upper (ventral) to 3.5 ml·min⁻¹·cm⁻³ in the lower (dorsal) lung regions, explaining 61% of the total variation within groups, whereas the horizontal gradient only explained 7% (right lung; supine subjects). Similar gravitational gradients were found in the single prone subject. \dot{V}_A and \dot{Q} were well matched except at the dorsal lung thoracic border where low values of \dot{V}_A/\dot{Q} due to a reduction in ventilation were occasionally found even in these normal subjects. V_B and \dot{Q} were reasonably well matched, implying that variations in vascular transit time due to gravity are kept to a minimum. The coefficient of local variation of peripheral vascular transit times (V_B/\dot{Q}) (33%) was, therefore, less than would have been expected if V_B and \dot{Q} were uncorrelated (57%).

regional ventilation-to-perfusion ratio; regional pulmonary hematocrit

MISMATCHING OF ventilation (\dot{V}_A) and perfusion (\dot{Q}) in normal lungs is quite modest (13, 18). Although hypoxic vasoconstriction may limit \dot{V}_A/\dot{Q} dispersion in diseased states (7), no study has convincingly shown the existence of hypoxic vasoconstriction in the normal supine lung breathing air. The mechanisms that lead to relative homogeneity of \dot{V}_A/\dot{Q} ratios in the gravitational axis in the normal lung are not fully understood.

In the companion paper (4) we showed that regional blood volume (V_B) might play a significant role in the determination of local alveolar expansion. A negative correlation between alveolar expansion and \dot{V}_A was found, consistent with an exponential pressure-volume curve first described by Salazar and Knowles (15). Thus, by virtue of its influence on regional expansion, vascular volume might be a determinant, indirectly, of \dot{V}_A .

To the extent that the regional distribution of \dot{Q} is associated with recruitment and distension of the vascular bed, increases in local \dot{Q} will correlate with increases in local vascular volume. Thus, under the influence of gravity, V_B may reduce the dispersion of \dot{V}_A/\dot{Q} in normal supine lung. Therefore, in this study, the relationship between regional \dot{Q} and regional V_B was studied in the supine lung, using positron emission tomography (PET).

With PET, \dot{Q} and volume are measured in absolute units under identical geometric conditions so that the dispersion of peripheral vascular transit times can be derived from the data for \dot{Q} and volume.

The paper concentrates on normal subjects in supine posture, but one prone subject was studied for comparison.

MATERIAL AND METHODS

Subjects

Eight healthy nonsmoking subjects were studied supine, and a different subject was studied prone; details are presented in a companion paper (4). The study was approved by the Hammersmith Hospital Research Ethics Committee and the United Kingdom Administration of Radioactive Substances Advisory Committee.

PET

Measurements were made by means of PET in a single transverse section of the thorax at midheart level, with a spatial resolution of 17 mm full width at half maximum. Regional lung density (D_L), regional alveolar gas volume (V_A), regional pulmonary V_B , regional extravascular lung tissue volume (V_{EV}), and regional \dot{V}_A were measured as previously described (5, 17). For the purpose of this study we also made measurements of regional \dot{V}_A/\dot{Q} on the same occasion.

\dot{V}_A/\dot{Q} . Measurements of \dot{V}_A/\dot{Q} were made with the constant infusion of the inert gas isotope ¹³N [half-life = 10 min; blood-to-gas partition coefficient (λ_N) = 0.015] dissolved in 0.9% saline (13, 14). During steady state, the delivery of tracer by the pulmonary circulation ($C_v\dot{Q}$) is balanced by the net removal of tracer by ventilation ($C_A\dot{V}_A$) and the small amount leaving the lung field in the efferent (downstream) blood ($\lambda_N C_A\dot{Q}$). Thus

$$\dot{V}_A/\dot{Q} = C_v/C_A - \lambda_N = V_A/(S_{13N}/C_v - 0.4V_B) - \lambda_N \quad (1)$$

where C_v and C_A are the mixed venous and alveolar concentrations of ¹³N, respectively, and \dot{Q} and \dot{V}_A are the gas-exchanging \dot{Q} and the ¹³N-transporting gas flow, respectively (both expressed per unit of thoracic volume). The operational equation is shown on the right, where S_{13N} is the regional ¹³N concentration per cubic centimeter of thorax. C_v was obtained from the tomogram, using a region corresponding to the right heart chamber. To obtain the amount of ¹³N in alveolar gas, ¹³N in the pulmonary blood pool must be accounted for. This was done assuming that 40% of the pulmonary V_B constitutes blood that has not yet equilibrated with alveolar gas (blood in pulmonary arteries and part of the capillaries). In the normal lung this correction does not exceed 15% of the ¹³N concentration (13). A 20% uncertainty in this correction would result in an error in \dot{V}_A/\dot{Q} of <3%.

\dot{Q} . \dot{Q} was calculated from the measurements of \dot{V}_A/\dot{Q} and \dot{V}_A by the relationship

$$\dot{Q} = \dot{V}_A/(\dot{V}_A/\dot{Q}) \quad (2)$$

When calculating \dot{Q} in this way, it should be emphasized that ventilation in the \dot{V}_A/\dot{Q} model, defined in terms of net removal of ¹³N from the blood (*Eq. 1*), may differ slightly from ventila-

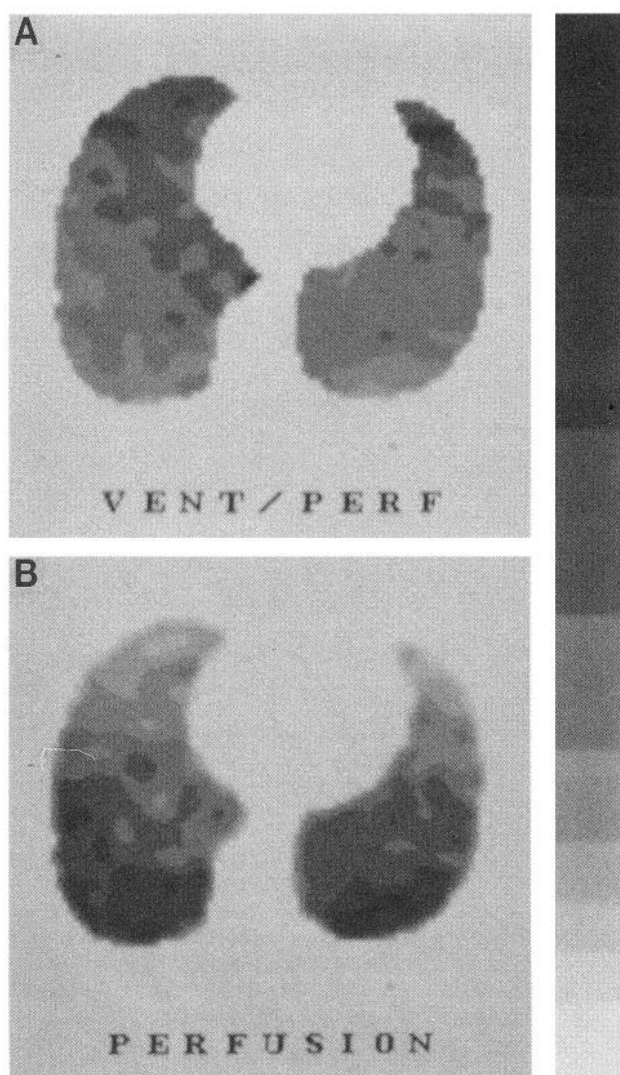


FIG. 1. Tomograms showing regional distribution of ventilation-to-perfusion ratio (Vent/Perf; \dot{V}_A/\dot{Q}) (A) and perfusion (\dot{Q} ; B) in 1 supine subject (same subject as shown in Fig. 2 of Ref. 4). Linear scale has been used with logarithmic shading. Top of scale is 2.5 for \dot{V}_A/\dot{Q} and 2.5 $\text{ml} \cdot \text{min}^{-1} \cdot \text{cm}^{-3}$ for \dot{Q} .

tion in the neon model, defined in terms of the delivery of tracer gas (^{19}Ne) to the alveoli (5).

Data Analysis and Error Considerations

The principles of data analysis are identical to those described previously (4). Vertical and horizontal profiles and interparametrical relationships were analyzed using values in $1.3 \times 1.3\text{-cm}$ square regions covering the lung fields. Only the right lung section was extensively analyzed, since it occupies approximately two-thirds of the total lung within the tomogram.

Statistics. The topographical (vertical and horizontal) variations of the parameters obtained were studied by the method of multiple regression in groups (8 subjects) using dummy variables (2). This enables the explained variation in relation to the within-group variation to be estimated as well as individual differences in regression parameters and mean values. $P > 0.05$ has been regarded nonsignificant, and $P < 0.001$ is the lowest level used. The correlation coefficients obtained were due to 1) common regression parameters ("slopes"), 2) individual "slopes," 3) vertical trends, and 4) horizontal trends and were calculated as $\sqrt{\text{explained variation}/\text{total variation within groups}}$. Significant levels were tested with F tests (2).

The relationship between V_B and \dot{Q} could not be explored directly, since values of V_B were used for the calculation of \dot{Q} . Even if the coupling is weak (an overestimation of V_B by 10% results in an underestimation of \dot{Q} by $\sim 2\%$), random errors in the measurements would affect the regression analysis between V_B and \dot{Q} . Instead, the relationship between V_A and $S_{13N}/C_{\dot{v}} - 0.4V_B$, which are independently measured, were explored (see Eq. 1). The relationship between V_B and \dot{Q} was then predicted from this relationship and the relationship between V_B and \dot{V}_A previously described (4) (i.e., $V_B = 0.16 + 0.27 \ln(\dot{V}_A) - 0.05\dot{V}_A$) and compared with observed values of the parameters. The correlation coefficients between observed and predicted values were calculated analogous to corresponding values by using multiple regression in groups (see above), i.e., 1) $R(\text{common}) = \sqrt{\text{explained variation due to common regression}/\text{total variation within groups}}$ and 2) $R(\text{individual}) = \sqrt{\text{explained variation due to individual regression}/\text{total variation within groups}}$. Data from the prone subject are dealt with separately.

Errors. Values of \dot{V}_A and \dot{V}_A/\dot{Q} suffer from a statistical uncertainty due to counting statistics in the measurements of radioactivity. For regions of the size of a resolution element ($1.7 \times 1.7\text{ cm}$), the coefficient of variation (CV) of \dot{V}_A is $\sim 5\text{--}6\%$ in the best-ventilated parts (17). The random errors of \dot{V}_A/\dot{Q} in the normal lung are on the order of 7–8% (14). The statistical errors of the calculated values of \dot{Q} thus range from 10% in ventral low-flow regions to 15% in dorsal high-flow regions.

Systematic errors due to simplifications in the underlying theories of the measurements of \dot{V}_A and \dot{V}_A/\dot{Q} are, in the normal lung, mainly caused by the effects of dead space ventilation. For the calculation of \dot{Q} , this results in an overestimation of \dot{Q} by $\sim 6\%$ in ventral parts of the lung in the supine posture and an underestimation by a similar number in dorsal parts (5).

RESULTS

Figure 1 shows images of regional \dot{V}_A/\dot{Q} (A) and the distribution of pulmonary \dot{Q} (B). Mean values of V_B , \dot{V}_A/\dot{Q} , and \dot{Q} calculated for the right lung field of each subject are presented in Table 1.

Crescent-shaped regions of low \dot{V}_A/\dot{Q} at the dorsal lung border were found in four of the eight subjects. Although clearly visible as high activity close to the chest wall in the ^{13}N scan, quantification of the \dot{V}_A/\dot{Q} ratio within these regions was not possible due to the limited spatial resolution. The crescents represent small regions of very low ventilation, as indicated by the slow ventilatory washout ($0.05\text{--}0.20\text{ min}^{-1}$) obtained by repeated to-

TABLE 1. Mean values of V_B , \dot{V}_A/\dot{Q} , and \dot{Q} calculated for right lung slice

Subj No.	V_B , ml/cm^3	\dot{V}_A/\dot{Q}	\dot{Q} , $\text{ml} \cdot \text{min}^{-1} \cdot \text{cm}^{-3}$
<i>Supine subjects</i>			
1	0.20	0.76	2.5
2	0.15	0.85	2.6
3	0.16	0.91	2.2
4	0.16	0.77	1.0
5	0.17	0.98	0.8
6	0.17	0.69	1.7
7	0.19	0.96	2.5
8	0.16	0.55	1.6
Mean	0.17	0.81	1.9
<i>Prone subject</i>			
	0.15	0.92	0.93

V_B , pulmonary blood volume; \dot{V}_A/\dot{Q} , alveolar ventilation-to-perfusion ratio; \dot{Q} , blood flow.

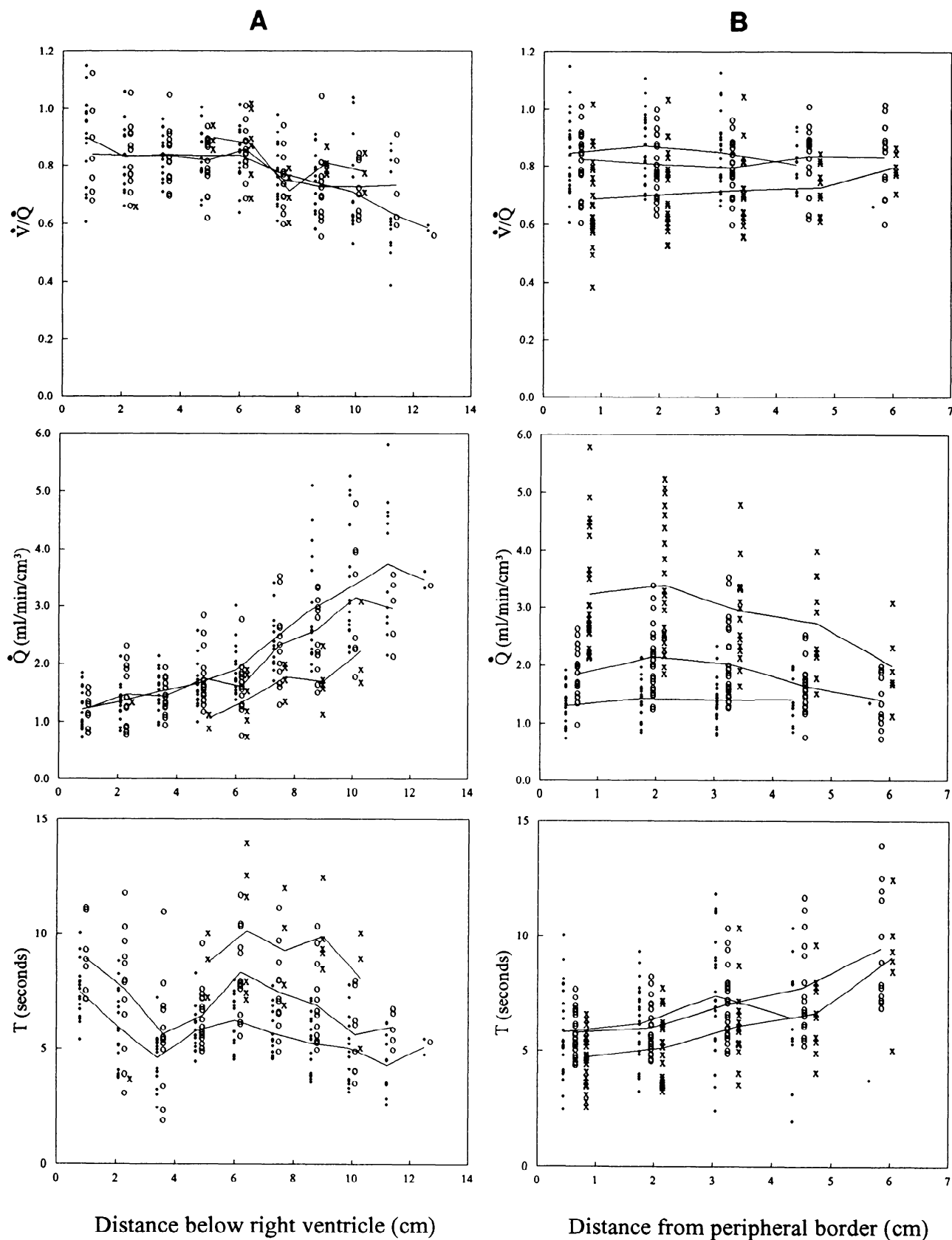


FIG. 2. Vertical (A) and horizontal (B) profiles of \dot{V}_A/\dot{Q} and \dot{Q} (right lung; $n = 267$) calculated for supine subjects. For each of 8 individuals, values were normalized to common mean calculated for all 8 subjects to exhibit vertical and horizontal trends. For each vertical level (A), data were separated into 3 subgroups: horizontal levels <2 cm from peripheral lung edge (solid circles), 2–5 cm (open circles), and >5 cm (crosses). Similarly, for each horizontal level (B), 3 subgroups were chosen: vertical levels <3 cm below right ventricle (solid circles), 3–7 cm (open circles), and >7 cm (crosses). Mean values for each subgroup and level are connected by straight lines. T , time.

TABLE 2. Relationships between various parameters (right lung) and vertical and horizontal levels

	\dot{V}_A/\dot{Q}	$\ln(\dot{Q})$
α	0.90	0.0
β of x_1	-0.02	0.1094
β of x_2		
$\beta(x_2)$		0.0988
$\beta(x_2^2)$		-0.0238
R^2 (common)	0.20	0.64
R^2 (individual)	0.53	0.78
r^2 (vertical)	0.20	0.61
r^2 (horizontal)		0.07

Values were from 8 supine subjects and were calculated by multiple regression in groups. Total number of regions is 267. α , Intercept; β , partial regression coefficient; R , multiple correlation coefficient, r , partial correlation coefficient; x_1 , cm below right ventricle; x_2 , cm from peripheral edge of lung. Note that the difference between R^2 (common) and R^2 (individual) is caused by differences in β values between subjects. Because of a small interdependence between x_1 and x_2 , sum of r^2 (vertical) and r^2 (horizontal) may exceed R^2 (common). $P < 0.001$ for all regression equations.

mograms immediately after the ^{13}N infusion was terminated.

Concerning the topographical distributions, there were no focal irregularities apart from these crescents. No significant differences in \dot{Q} or \dot{V}_A/\dot{Q} were found between the right and the left lung (differences were $<4\%$).

Vertical and Horizontal Gradients

Supine subjects. On average there was an increase in \dot{Q} by 11%/cm vertical distance in the direction of gravity (Fig. 2), explaining 61% of the total within-groups variation (Table 2). The profile was similar in shape to that of \dot{V}_A (4), although slightly steeper. The greater vertical gradient in \dot{Q} compared with that in \dot{V}_A resulted in falling values of the \dot{V}_A/\dot{Q} ratio from 0.9 ventrally to 0.7 dorsally. Even though the vertical \dot{V}_A/\dot{Q} gradient reached significance for the group as a whole, the \dot{V}_A/\dot{Q} profile was rather flat and three subjects even had slightly rising profiles. No statistically significant horizontal gradients of \dot{V}_A/\dot{Q} were found (Fig. 2). There was a small horizontal gradient of regional \dot{Q} (Fig. 2), but this only explained 7% of the variation (Table 2).

Prone subject. The vertical gradients of \dot{V}_A/\dot{Q} and \dot{Q} showed similar trends in the axis of gravity for the supine subjects (Fig. 3), although \dot{V}_A/\dot{Q} fell more rapidly from upper to lower lung regions ($P < 0.001$ for both parameters). No significant horizontal gradients were seen.

Interparametrical Relationships

Because of the mathematical coupling between \dot{Q} and V_B (although small), the relationship between the two parameters was initially explored by first observing the relationship between \dot{V}_A and $S_{13\text{N}}/C_{\dot{v}} - 0.4V_B$ (Eq. 1), and no correlation was found in either the supine (Fig. 4A) or the prone posture. This means that \dot{V}_A/\dot{Q} is proportional to \dot{V}_A (see Eq. 1), and, since $\dot{Q} = \dot{V}_A/(\dot{V}_A/\dot{Q})$ (Eq. 2), it follows that \dot{Q} is proportional to \dot{V}_A/V_A . However, we have previously calculated the predicted equations for the relationships between V_B , V_A , and \dot{V}_A (4) (same sub-

jects on same occasion). This allows the predicted relationship between \dot{Q} and V_B to be calculated (Fig. 4B), giving values of R^2 (common) = 0.48 and R^2 (individual) = 0.48 ($P < 0.001$; supine subjects). For the single prone subject ($n = 42$), $r^2 = 0.48$ ($P < 0.001$). In other words, CV of regional transit time (V_B/\dot{Q}) from the individual regions shown in Fig. 4B, 33%, is much smaller than 57% that would have been expected if the two parameters were uncorrelated (CV for $\dot{Q} = 47\%$ and for $V_B = 32\%$, giving CV for $V_B/\dot{Q} = \sqrt{0.47^2 + 0.32^2}$; supine subjects; normalized data).

DISCUSSION

The range of the average regional pulmonary \dot{Q} between subjects ($0.8\text{--}2.6 \text{ ml} \cdot \text{min}^{-1} \cdot \text{cm}^{-3}$; Table 1) may seem surprisingly high, but cardiac output in normal supine subjects can vary by almost a factor of three between subjects (10). The wide range in \dot{Q} is mainly due to low values of \dot{Q} in subjects 4 and 5, who also exhibit rather low values of \dot{V}_A (on average $0.8 \text{ ml} \cdot \text{min}^{-1} \cdot \text{cm}^{-3}$ for right lung), resulting in normal \dot{V}_A/\dot{Q} values.

It should be noted that \dot{V}_A and \dot{V}_A/\dot{Q} measurements were performed consecutively and that ventilation might have been lower during the measurement of \dot{V}_A than \dot{V}_A/\dot{Q} , in which case \dot{Q} is underestimated. However, the relative distribution of the values of \dot{Q} obtained should not be affected unless the distribution of gas flow changes along with these relatively small variations in minute ventilation.

Low values of \dot{V}_A/\dot{Q} were found at the dorsal lung thoracic border (crescents) in one-half of the subjects studied, and the occurrence of these regions was not related to physical condition, sex, height, or weight. These crescents were too narrow and too close to the thoracic wall to allow quantification of \dot{V}_A/\dot{Q} , as they were located within the peripheral 2 cm of the lung exempted from

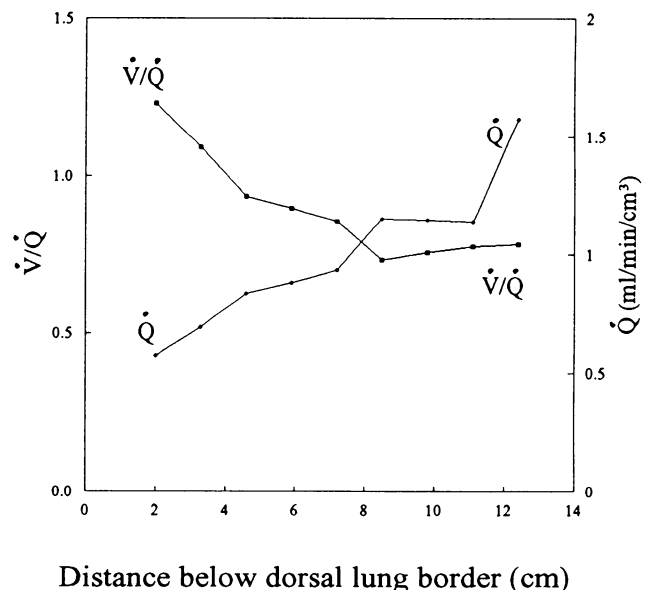


FIG. 3. Vertical profiles of \dot{V}_A/\dot{Q} and \dot{Q} calculated for prone subject. Only mean values at each vertical level are shown and are connected by straight lines.

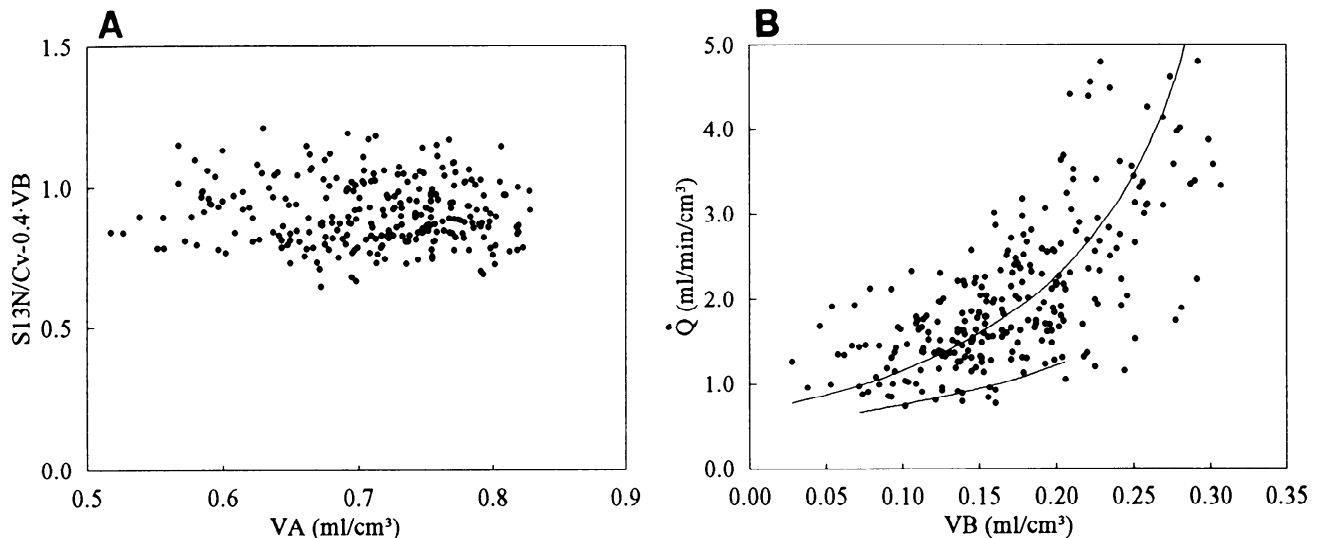


FIG. 4. *A*: primary analysis of normalized data revealed no association between independently measured parameters alveolar volume (V_A) and $S_{13N}/C_v - 0.4V_B$, where S_{13N} is pulmonary concentration of ^{13}N from emission scans, C_v is mixed venous concn, and V_B is pulmonary blood volume. *B*: relationships between \dot{Q} and V_B . Plotted values of \dot{Q} are normalized to group mean ($1.9 \text{ ml} \cdot \text{min}^{-1} \cdot \text{cm}^{-3}$; 8 subjects, right lung; $n = 267$), but regression equations are derived from nonnormalized data. Regression curve for prone subject is also shown (bottom line). See text for details.

analysis. Similar crescents have been seen in other healthy subjects when infused ^{13}N was used (13). Thus, small regions of lung with very low ventilation, but with an unimpeded \dot{Q} , commonly exist in the most dependent parts of the lung in normal subjects. Such regions were not visible in ventilation measurements using ^{19}Ne or in measurements of D_L , which suggests that the size is well below the spatial resolution of the tomograph.

Vertical and Horizontal Gradients

Regional \dot{Q} increases similarly to \dot{V}_A in the direction of gravity in a number of different body positions (for review, see Ref. 1), and the gradient is most pronounced in the erect posture. With regard to supine and prone subjects, however, uniform distributions of \dot{Q}/V_A and $\dot{Q}/\text{alveolus}$ have been reported (1, 12).

In this study the vertical gradient in \dot{Q} per unit volume of thorax, in the supine subjects as well as the single prone subject, is substantially larger than earlier reported values obtained using ^{133}Xe or ^{81m}Kr . \dot{V}_A and \dot{Q} follow each other in a tightly linked fashion, giving a relatively constant \dot{V}_A/\dot{Q} ratio. When ^{99m}Tc -labeled microspheres were used, large horizontal \dot{Q} gradients were reported (8). We could not confirm this, although the peripheral 2 cm of the lung had to be excluded from analysis due to the limited resolution of the tomograph.

\dot{Q} and V_B . V_B and \dot{Q} appear to be reasonably well matched in the normal lung (Fig. 4*B*). If recruitment alone were responsible for the gravitational increase in \dot{Q} , the relationship between V_B and \dot{Q} would have been expected to be linear. Vascular compliance and resistance are almost uniformly distributed between pulmonary arteries and veins (11, 16). The shape of the V_B - \dot{Q} curve in Fig. 4*B* thus suggests that distension ($\dot{Q} \sim V_B^2$ for laminar flow) of resistance vessels at increasing trans-

vascular pressure plays a significant role, at least in regions where the V_B is high, i.e., in the dorsal parts of the lung. Thus, under the influence of gravity the distribution of vascular volume plays a role in matching \dot{V}_A to \dot{Q} . The increase in \dot{Q} in the dependent regions of the lung is associated with vascular distension and recruitment. This increase in V_B correlates inversely with V_A , partly because of the competition for space per cubic centimeter of thorax but mostly because vascular weight is the most important mechanical force distorting the lung parenchyma. V_A is itself inversely proportional to \dot{V}_A and might act as a link between vascular volume and \dot{V}_A whereby the dispersion of \dot{V}_A/\dot{Q} is diminished.

Although not a perfect match, the positive correlation between V_B and \dot{Q} (Fig. 4*B*), which was found in both supine and prone postures, is of importance in reducing intraregional variation of vascular transit times. Our data from 1.3×1.3 -cm regions show that the CV of V_B/\dot{Q} is 33% compared with the expected 57%, which would have been the case if V_B and \dot{Q} were uncorrelated. It is necessary to distinguish red blood cell, plasma, and whole blood transit times, as well as total transit (capillaries plus larger vessels) vs. capillary transit times. Regional transit times are only of physiological relevance in relation to capillary transit times that we have discussed elsewhere (3). On the assumption that mean values for the right lung slice are representative for the lung as a whole, the intrapulmonary mean transit time for whole blood (total V_B divided by total \dot{Q}) averages 5.4 s (using mean values of V_B and \dot{Q} from Table 2). We have previously argued (6) that capillary volume is $\sim 25\%$ of the total pixel V_B , which would give a capillary transit time from our data of $\sim 5.4 \times 0.25 = 1.3$ s. Because the capillary hematocrit is $\sim 60\%$ of that in larger vessels (6), red blood cell transit time will be $0.6 \times 1.3 = 0.8$ s, which is in line with red blood cell capillary transit in humans measured with the Roughton-Forster technique (9).

We thank D. D. Vonberg and the staff of the Cyclotron Unit, in particular P. D. Buckingham of the radiochemistry section, for invaluable support and technical and intellectual help and all our volunteers. Professor B. Jonson (University of Lund) gave much helpful advice in the preparation of this paper.

This study was supported in part by the Draco Foundation, Thorsten Birger Segerfalks Foundation for Medical Research and Education, Swedish National Association Against Heart Diseases, and Swedish Medical Research Council Grant 02872.

Present address and address for reprint requests: L. H. Brudin, Dept. of Clinical Physiology, Kalmar Hospital, S-391 85 Kalmar, Sweden.

Received 6 April 1992; accepted in final form 12 October 1993.

REFERENCES

1. **Amis, T. C., H. A. Jones, and J. M. B. Hughes.** Effect of posture on inter-regional distribution of pulmonary perfusion and \dot{V}_A/\dot{Q} ratios in man. *Respir. Physiol.* 56: 169-182, 1984.
2. **Armitage, P.** *Statistical Methods in Medical Research.* London: Blackwell, 1983.
3. **Brudin, L. H.** *Topography of Pulmonary Structure and Function in Man Using Positron Emission Tomography (PET)* (PhD thesis). University of Lund, Sweden: University of Lund, 1992.
4. **Brudin, L. H., C. G. Rhodes, S. O. Valind, T. Jones, B. Jonson, and J. M. B. Hughes.** Relationships between regional ventilation and vascular and extravascular volume in supine man. *J. Appl. Physiol.* 76: 1195-1204, 1994.
5. **Brudin, L. H., S. O. Valind, and C. G. Rhodes.** Error analysis of combined measurements of regional ventilation and \dot{V}/\dot{Q} ratio using positron emission tomography. *Phys. Med. Biol.* 37: 1077-1093, 1992.
6. **Brudin, L. H., S. O. Valind, C. G. Rhodes, D. R. Turton, and J. M. B. Hughes.** Regional lung hematocrit in humans using positron emission tomography. *J. Appl. Physiol.* 60: 1155-1163, 1986.
7. **Grover, R. F., W. W. Wagner, Jr., I. F. McMurtry, and J. T. Reeves.** Pulmonary circulation. In: *Handbook of Physiology. The Cardiovascular System. Peripheral Circulation and Organ Blood Flow.* Bethesda, MD: Am. Physiol. Soc., 1983, sect. 2, vol. III, pt. 1, chapt. 4, p. 103-136.
8. **Hakim, T. S., R. Lisbana, and G. W. Dean.** Gravity-independent inequality in pulmonary blood flow in humans. *J. Appl. Physiol.* 63: 1114-1121, 1987.
9. **Johnson, R. L., Jr., W. S. Spicer, J. M. Bishop, and R. E. Forster.** Pulmonary capillary blood volume, flow, and diffusing capacity during exercise. *J. Appl. Physiol.* 15: 893-902, 1960.
10. **Nyström, J., F. Celsing, P. Carlens, B. Ekblom, and P. Ring.** Evaluation of a modified acetylene rebreathing method for the determination of cardiac output. *Clin. Physiol. Oxf.* 6: 253-268, 1986.
11. **Permutt, S., and R. G. Brower.** Mechanical support. In: *The Lung: Scientific Foundations*, edited by R. G. Crystal, J. B. West, P. J. Barnes, N. S. Cherniack, and E. R. Weibel. New York: Raven, 1991, p. 1079-1080.
12. **Prefaut, C. H., and L. A. Engel.** Vertical distribution of perfusion and inspired gas in supine man. *Respir. Physiol.* 43: 209-219, 1981.
13. **Rhodes, C. G., S. O. Valind, L. H. Brudin, P. E. Wollmer, T. Jones, P. D. Buckingham, and J. M. B. Hughes.** Quantification of the regional \dot{V}/\dot{Q} ratio in man using positron emission tomography. II. Procedure and normal values. *J. Appl. Physiol.* 66: 1905-1913, 1989.
14. **Rhodes, C. G., S. O. Valind, L. H. Brudin, P. E. Wollmer, T. Jones, and J. M. B. Hughes.** Quantification of the regional \dot{V}/\dot{Q} ratio in man using positron emission tomography. I. Theory. *J. Appl. Physiol.* 66: 1896-1904, 1989.
15. **Salazar, E., and J. H. Knowles.** An analysis of pressure-volume characteristics of the lungs. *J. Appl. Physiol.* 19: 97-104, 1964.
16. **Taylor, A. E., J. W. Barnard, S. A. Barman, and W. K. Adkins.** Fluid balance. In: *The Lung: Scientific Foundations*, edited by R. G. Crystal, J. B. West, P. J. Barnes, N. S. Cherniack, and E. R. Weibel. New York: Raven, 1991, p. 1148-1150.
17. **Valind, S. O., C. G. Rhodes, L. H. Brudin, and T. Jones.** Measurements of regional ventilation pulmonary gas volume: theory and error analysis, with special reference to positron emission tomography. *J. Nucl. Med.* 32: 1937-1944, 1991.
18. **Wagner, P. D., R. B. Laravuso, R. R. Uhl, and J. B. West.** Continuous distributions of ventilation-perfusion ratios in normal subjects breathing air and 100% O₂. *J. Clin. Invest.* 54: 54-68, 1974.